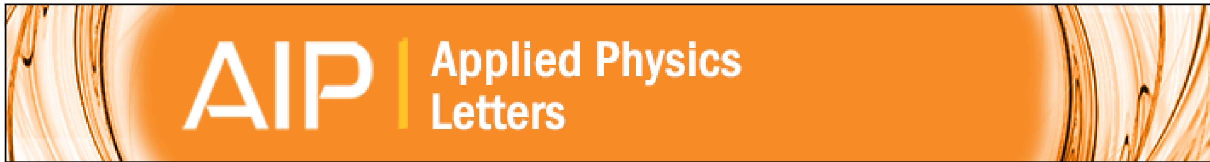

Transmission electron microscopy and photoluminescence studies of Er implanted low-temperature grown GaAs:Be

R. L. Maltez, Z. Liliental-Weber, J. Washburn, M. Behar, P. B. Klein, P. Specht, and E. R. Weber

Citation: Applied Physics Letters **73**, 2170 (1998); doi: 10.1063/1.122412
View online: http://dx.doi.org/10.1063/1.122412
View Table of Contents: http://scitation.aip.org/content/aip/journal/apl/73/15?ver=pdfcov
Published by the AIP Publishing

Articles you may be interested in

Transition of electron transport process in Be-doped low-temperature-grown GaAs layer
J. Appl. Phys. **114**, 083716 (2013); 10.1063/1.4819902

Cooperative transition of electronic states of antisite As defects in Be-doped low-temperature-grown GaAs layers
J. Appl. Phys. **110**, 123716 (2011); 10.1063/1.3671059

Direct exchange interaction of localized spins associated with unpaired sp electrons in Be-doped low-temperature-grown GaAs layers
J. Appl. Phys. **109**, 073918 (2011); 10.1063/1.3567914

Structural and photoluminescence studies of Er implanted Be doped and undoped low-temperature grown GaAs
J. Appl. Phys. **85**, 1105 (1999); 10.1063/1.369236

Two-dimensional arsenic precipitation in superlattice structures of alternately undoped and heavily Be-doped GaAs grown by low-temperature molecular beam epitaxy
Appl. Phys. Lett. **72**, 1984 (1998); 10.1063/1.121240

NEW Special Topic Sections
NOW ONLINE
Lithium Niobate Properties and Applications: Reviews of Emerging Trends
AIP Applied Physics Reviews

Reuse of AIP Publishing content is subject to the terms at: https://publishing.aip.org/authors/rights-and-permissions. Download to IP: 143.54.44.137 On: Thu, 05 May 2016 20:00:57

Transmission electron microscopy and photoluminescence studies of Er implanted low-temperature grown GaAs:Be

R. L. Maltez,[a] Z. Liliental-Weber,[b] and J. Washburn
Materials Science Division, Lawrence Berkeley Laboratory, University of California, Berkeley, California 94720

M. Behar
Instituto de Física, UFRGS, Porto Alegre, RS, Brazil 91501-970

P. B. Klein
Naval Research Laboratory, Washington, DC 20375-5347

P. Specht and E. R. Weber
University of California, Department of Material Science, Berkeley, California 94720

(Received 6 April 1998; accepted for publication 14 August 1998)

Characteristic 1.54 μm $4f$-$4f$ emission has been observed from Er^{3+} centers in Er-implanted and annealed, low-temperature grown GaAs:Be samples, while cross-sectional transmission electron microscopy (TEM) studies reveal very little structural damage for elevated temperature implants. No Er emission was observed from any of the as-implanted samples, while the Er emission intensity was significantly more intense after 650 °C anneals than after 750 °C anneals. Significant enhancement of the optically active Er incorporation was achieved when the implantation was carried out at 300 °C. For the two total Er fluences employed (5.5×10^{13} and 13.6×10^{13} Er/cm^2) the Er emission intensity exhibited a linear dependence upon implantation fluence, while TEM indicated no significant increase in the damage level at the higher fluence 300 °C implant. © *1998 American Institute of Physics.* [S0003-6951(98)04641-5]

Rare earth (RE) doped III–V semiconductors have been a subject of great interest in recent years because of their potential to emit spectrally sharp, temperature stable, and host independent luminescence. Such a light source would have applications in semiconductor light-emitting diodes (LEDs), lasers, and as components for optical communication technology. In particular for Er, the internal $4f$ transition from the first excited state to the ground state ($^4I_{13/2}\rightarrow{}^4I_{15/2}$) results in a photon emission near 1.54 μm. This is an important wavelength because it corresponds to the minimum absorption in standard silica-based optical fibers.[1,2]

Such characteristic Er emission has already been observed for standard GaAs hosts doped with Er by different procedures,[1,3–5] and for other technologically important semiconductors such as Si,[2] AlGaAs,[5] InP, and GaP.[1] The nature of the Er radiative center in GaAs is not yet clear[3–6] and it is likely that the dominant Er site is growth dependent and can differ for molecular beam epitaxy (MBE) and metal organic chemical vapor deposition (MOCVD) materials. In the same way, Er doping by ion implantation or directly during growth may result in different sites for kinetic reasons. The purpose of this study is to implant Er into low temperature grown GaAs (LT-GaAs)[7] to verify the possibility of a sharp and temperature stable light emission from a short carrier lifetime material. Be doped LT-GaAs has some further advantages over the undoped material. Be doping strongly suppresses As precipitation after annealing.[8] Also, samples grown at temperatures as high as 300 °C show the same short photocarrier lifetime that is only obtained for undoped LT-GaAs grown at ~200 °C.[8] In this work we show, for the first time, that the characteristic Er photoluminescence (PL) is obtained when Er atoms are incorporated into LT-GaAs:Be by ion implantation. We also show that it is possible to strongly minimize implantation damage and increase considerably the Er emission by keeping the sample at 300 °C during the implantation procedure.

A Be doped LT-GaAs layer ([Be]$=7\times10^{19}$ cm^{-3}) 1.5 μm thick was grown by MBE on a (001) GaAs substrate at 300 °C with a fixed As/Ga beam equivalent pressure ratio of 20. Wafers were Er implanted at room temperature (RT) and at 300 °C at an energy of 450 keV to a fluence of 5.5×10^{13} Er/cm^2. The Er peak concentration is calculated as 6.5×10^{18} Er/cm^3, almost 10 times higher than the Er solubility observed for GaAs.[9] A plateau Er implant with a broader depth distribution was also performed, but only at 300 °C implantation temperature. For this special case, three consecutive Er implants were performed at energies of 480, 155, and 40 keV to fluences of 9.4×10^{13}, 3.1×10^{13}, and 1.1×10^{13} Er/cm^2, respectively, i.e., to a total fluence of 13.6×10^{13} Er/cm^3. These implantation parameters were projected to result in an almost flat Er concentration of 1×10^{19} Er/cm^3 from 10 to 145 nm, based on each individual profile as calculated by the TRIM[10] program. Rapid thermal annealings (RTA) for 30 s at 650 °C and at 750 °C were also performed.

The structural quality of the layers was investigated using a Topcon 002B transmission electron microscope. Cross-sectional specimens were prepared by mechanical polishing and dimpling, followed by ion milling on a liquid nitrogen-cooled stage. PL measurements were performed at 10 K using 514 nm excitation from an argon ion laser. The emitted

[a] Postdoctoral fellowship by CAPES-Brasília/Brasil.
[b] Electronic mail: zlw@ux5.lbl.gov

Reuse of AIP Publishing content is subject to the terms at: https://publishing.aip.org/authors/rights-and-permissions. Download to IP: 143.54.44.137 On: Thu, 05 May 2016 20:00:57

 © 1998 American Institute of Physics

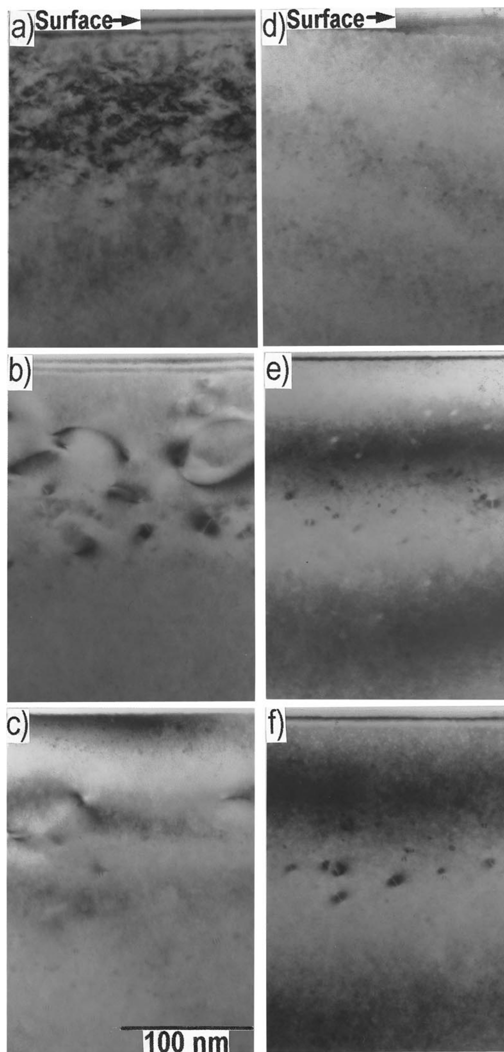

FIG. 1. Cross-sectional TEM micrographs (BF $0\bar{2}2$) for single Gaussian implant at room temperature (RT) and plateau implantation at 300 °C. The (001) surface is the top edge of each figure. Pictures (a), (b), and (c) correspond to the single implant performed at RT, (d), (e), and (f) correspond to the implantation performed at 300 °C. The first picture [(a) or (d)] is the observation from the as-implanted sample, the second one [(b) or (e)] is after the 650 °C anneal, and the last one [(c) or (f)] is after the 750 °C anneal.

radiation was collected and analyzed with a 0.22 m double grating spectrometer, and the PL signal was detected by a liquid nitrogen-cooled germanium detector using standard synchronous detection techniques.

Figure 1 shows TEM micrographs from the single implant at RT [Figs. 1(a), 1(b), and 1(c)] and the plateau implantation at 300 °C [Figs. 1(d), 1(e), and 1(f)]. We do not show the TEM results of the single implant at 300 °C since they are quite similar to the ones corresponding to the plateau implantation at 300 °C. All of these are cross-sectional images in bright field (BF) taken with $\mathbf{g}=0\bar{2}2$. The (001) sample surface is shown at the top of each figure. As can be seen in Fig. 1, the single implant at RT [Fig. 1(a)] produces the strongest damage, but the sample is still crystalline due to the low implantation fluence. Figure 1(d) is an image taken from plateau implanted sample at 300 °C. The implantation at high temperature results in a strong improvement in the sample's crystalline quality as almost no defects are visible by TEM.

TABLE I. Estimates for the total extension of dislocation lines per unit volume of the sample.

	$\overline{2r}\pi\nu_1$ (cm^{-2})		
RTA	Gaussian RT	Gaussian 300 °C	Plateau 300 °C
650 °C	2.8×10^{10}	1.5×10^{9}	2.3×10^{9}
750 °C	1.6×10^{10}	0.9×10^{9}	2.2×10^{9}

Figures 1(b) and 1(e) are micrographs from 650 °C annealed samples. Figure 1(b) shows dislocation loops (mean diameter $\overline{2r}\sim 15$ nm) extending almost from the surface to the depth of approximately 160 nm. The plateau implanted sample at 300 °C [Fig. 1(e)] shows much smaller ($\overline{2r}\sim 1.5$ nm) dislocation loops than for the RT case. The dislocation loop density (ν_1) is about the same: $(6\pm2)\times10^{-6}$ loops/nm^3, for RT, and $(5\pm2)\times10^{-6}$ loops/nm^3, for 300 °C implantations.

Figures 1(c) and 1(f) are micrographs from 750 °C annealed samples. They show a decrease in the density of dislocation loops: $\nu_1=(2\pm1)\times10^{-6}$ loops/nm^3 for both cases. The RT implanted sample is now almost free of dislocations in the near surface area down to around 60 nm. From 60 nm to about 110 nm some large loops, $\overline{2r}\sim 25$ nm, are observed (end of range defects). For the plateau implantation at 300 °C [Fig. 1(f)], the loops observed at the end of range area (around 130 nm) are much smaller, $\overline{2r}\sim 3.5$ nm. Table I shows estimates, from TEM micrographs, for the quantity $\overline{2r}\pi\nu_1$, which represents the total length of dislocation lines per unit volume. This factor estimates the crystalline quality (from the point of view of extended defects) for each sample, demonstrating that a large fraction of the ion damage has continuously recovered during implantation at 300 °C.

Annealing of LT-GaAs:Be layers at 650 °C did not lead to the formation of As precipitates. However, such precipitates were observed below the implanted area after annealing at 750 °C. Within the implanted area, after 750 °C annealing, a different type of precipitate was observed. From contrast analysis under dark field image conditions taken with $\mathbf{g}=200$, they appear to be ErAs precipitates.[9,6] They show an intense bright contrast under this image condition and are completely coherent with the matrix. The details of these studies will be described elsewhere.[11]

Figure 2 shows PL spectra comparing results from the single implant performed at RT (full lines) to the single implant performed at 300 °C (points). The measurements were performed on as-implanted, annealed at 650 and at 750 °C samples. As can be seen in Fig. 2, the emission in that spectral range is dominated by a very broad background signal, which increases monotonically with the annealing temperature and is also stronger for 300 °C implantation than for RT implantation. Thus the PL background is increasing with improving crystalline quality. However, the factors of 2–3 increase in the background PL between 650 and 750 °C anneal temperatures (Fig. 2) do not appear to correlate well with decreases in the dislocation line density $\overline{2r}\pi\nu_1$, which only exhibits a small to modest reduction (5%–45%, Table I) over this temperature range. It is clear that the increase in the background PL must involve a decrease in the concentration of localized defects as well as the extended defects. A comparison of the background PL spectrum with that of typical

Reuse of AIP Publishing content is subject to the terms at: https://publishing.aip.org/authors/rights-and-permissions. Download to IP: 143.54.44.137 On: Thu, 05 May 2016 20:00:57

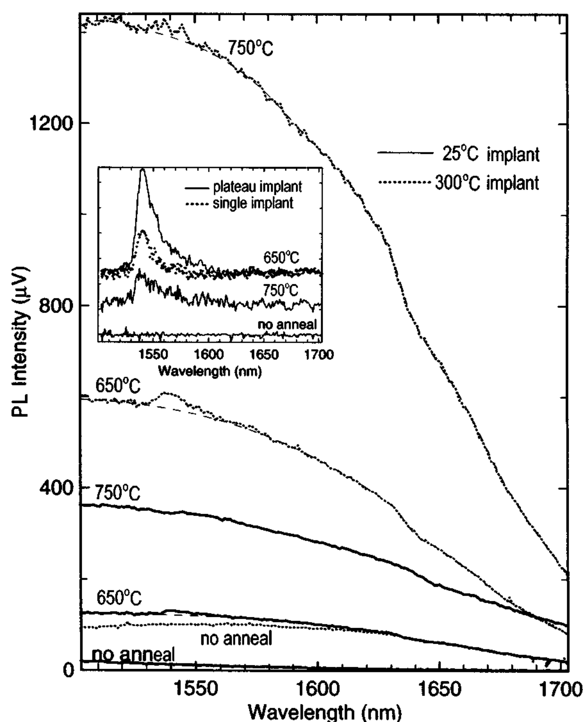

FIG. 2. PL spectra comparing the single implant performed at RT (full lines) to the single implant performed at 300 °C (points), for the as-implanted, 650 °C annealed, and 750 °C annealed samples. Insert: PL spectra with background subtraction from plateau implanted samples before and after annealing (full lines) and also from the single implant at 300 °C subsequently annealed at 650 °C (points).

semi-insulating GaAs samples[12] suggests that this PL is most probably due to the broad 0.8 eV band, which has been associated with microdefect formation[12] better than the 0.65 eV As_{Ga} (EL2) emissions bands. The background PL observed in this study exhibits a long, high energy tail that extends essentially up to the band gap.

However, the most interesting feature in Fig. 2 is the 1.54 μm Er emission. This is found to be considerably stronger for implantation performed at 300 °C. It is also found significantly more intense for annealing at 650 °C than at 750 °C, which is a similar temperature behavior to that observed for standard GaAs samples,[1] where the optimum case was near 650 °C. No Er emission is observed from the as-implanted samples or from the RT implanted sample annealed at 750 °C. While the Er^{3+} emission spectrum usually consists of a series of sharp lines, it has been observed that in standard GaAs (as well as other semiconductors) the Er emission from certain sites tends to be significantly broadened,[3] appearing very similar to the Er spectra in Fig. 2. Apparently this site occurs in several slightly differing environments, thus leading to a smearing of the crystal field-split emission lines. The insert in Fig. 2 shows the PL spectra (after background subtraction) obtained from plateau implanted samples (full lines). These spectra also exhibit the strongest Er signal after 650 °C annealing. However, the intensity is higher for the plateau implanted samples because of the higher total Er fluence. For comparison purposes, the PL spectrum (with background subtraction) from single implant at 300 °C and annealed at 650 °C is included (points) in the insert. A single/plateau Er emission ratio of 0.41 can be observed which agrees fairly well with the expected ratio of 0.4 between the implantation fluences employed for each case.

The observed intensity of the characteristic Er emission obtained after 650 °C annealing indicates that a significant concentration of optically active Er sites was achieved. The optically active center has been suggested to be the Er tetrahedral interstitial site.[3,5] The strong decrease in the 1.54 μm Er emission observed after 750 °C annealing, while the background PL is continuing to increase, indicates that the optically active Er sites have become thermally unstable. We also begin to observe some ErAs precipitation[11] at this annealing temperature. These two observations suggest the possibility that instead of having a high concentration of isolated Er interstitials in the GaAs matrix, we now have a high concentration of Er–As complexes. These complexes could be the initial step before the beginning of ErAs precipitation. The following two facts also support this picture: Er tetrahedral interstitial sites are a natural precursor for ErAs precipitation,[6] and the Er was incorporated into the matrix as a supersaturated solution.[9]

In summary, in the present work we have shown for the first time that it is possible to observe the 1.54 μm Er emission in LT-GaAs:Be samples. The emitting Er centers appear to be thermally activated with the 650 °C annealing temperature being far more efficient, for their activation, than 750 °C annealing. Implantation at 300 °C shows very few extended defects and also results in a considerably higher PL intensity (for the Er and background PL) than for Er implants carried out at room temperature. The PL intensity was also found to scale with the implantation fluence, suggesting that the Er PL intensity might be increased further by performing Er implants at higher fluences.

This work was supported by AFOSR-ISSA-90-0009. The use of facilities of the National Center for Electron Microscopy at Lawrence Berkeley National Laboratory is very much appreciated.

[1] G. S. Pomrenke, H. Ennen, and W. Haydl, J. Appl. Phys. **59**, 601 (1986).
[2] A. Polman, J. Appl. Phys. **82**, 1 (1997).
[3] P. B. Klein, F. G. Moore, and H. B. Dietrich, Appl. Phys. Lett. **58**, 502 (1991).
[4] K. Takahei, A. Taguchi, Y. Horikoshi, and J. Nakata, J. Appl. Phys. **76**, 4332 (1994).
[5] D. W. Elsaesser, J. E. Colon, Y. K. Yeo, R. L. Hengehold, K. R. Evans, and J. S. Solomon, J. Cryst. Growth **127**, 707 (1993).
[6] J. Nakata, N. Jourdan, H. Yamaguchi, K. Takahei, Y. Yamamoto, and Y. Kido, J. Appl. Phys. **77**, 3095 (1995).
[7] *Low Temperature (LT) GaAs and Related Materials*, edited by G. L. Witt, R. Calawa, U. Mishra, and E. Weber (Material Research Society, Pittsburgh, 1991), Vol. 241; F. W. Smith, *ibid.*, p. 3.
[8] P. Specht, S. Jeong, H. Sohn, M. Luysberg, A. Prasad, J. Gebauer, R. Krause-Rehberg and E. R. Weber, International Conference on Defects in Semiconductors Proceedings, ICDS 19, Aveiro, Portugal, 1997 (unpublished).
[9] I. Poole, K. E. Singer, and A. R. Peaker, J. Cryst. Growth **121**, 121 (1992).
[10] J. F. Ziegler, J. P. Biersack, and U. Littmark, *The Stopping and Range of Ions in Solids* (Pergamon, Oxford, 1985), Vol. 1.
[11] R. L. Maltez, Z. Liliental-Weber, J. Washburn, M. Behar, P. B. Klein, P. Specht, and E. R. Weber (unpublished).
[12] M. Tajima, Jpn. J. Appl. Phys., Part 2 **21**, L227 (1982).

Reuse of AIP Publishing content is subject to the terms at: https://publishing.aip.org/authors/rights-and-permissions. Download to IP: 143.54.44.137 On: Thu, 05 May 2016 20:00:57